Journal of Analytical Science and Technology

RESEARCH ARTICLE Open Access

Electrochemical investigations and theoretical studies of biocompatible niacin-modified carbon paste electrode interface for electrochemical sensing of folic acid

Pattan-Siddappa Ganesh[1], Sang-Youn Kim[1*], Dong-Soo Choi[2], Savas Kaya[3*], Goncagül Serdaroğlu[4], Ganesh Shimoga[1], Eun-Jae Shin[1] and Seok-Han Lee[1]

Abstract

The modified electrode–analyte interaction is critical in establishing the sensing mechanism and in developing an electrochemical sensor. Here, the niacin-modified carbon paste electrode (NC/CPE) was fabricated for electrochemical sensing applications. The two stable structures of the niacin were optimized and confirmed by the absence of negative vibrational frequency, at B3LYP and B3LYP-GD3BJ level and 6–311 g** basis set. The physical and quantum chemical quantities were used to explain the molecular stability and electronic structure-related properties of the niacin. The natural bond orbital (NBO) analysis was performed to disclose the donor–acceptor interactions that were a critical role in explaining the modifier–analyte interaction. The fabricated NC/CPE was used for the determination of folic acid (FA) in physiological pH by cyclic voltammetry (CV) method. The limit of detection (LOD) for FA at NC/CPE was calculated to be 0.09 µM in the linear concentration range of 5.0 µM to 45.0 µM (0.2 M PBS, pH 7.4) by CV technique. The analytical applicability of the NC/CPE was evaluated in real samples, such as fruit juice and pharmaceutical sample, and the obtained results were acceptable. The HOMO and LUMO densities are used to identify the nucleophilic and electrophilic regions of niacin. The use of density functional theory-based quantum chemical simulations to understand the sensory performance of the modifier has laid a new foundation for fabricating electrochemical sensing platforms.

Keywords: Niacin, Electrochemical sensor, Natural bond orbital, Carbon paste electrode, Conceptual density functional theory, Real sample analysis

Background

The analysis and determination of pharmaceutical compounds plays a key role in examining its purity and possible consequences on the treatment method (Afshar et al. 2020). Folic acid (FA) is an important water-soluble vitamin and an essential hematogenic agent which acts as coenzyme to regulate the generation of ferroheme (Kingsley et al. 2015). It also helps in the synthesis and methylation of DNA (D'Souza et al. 2017). Deficiency of FA can cause severe health issues like neurosis, gigantocytic

*Correspondence: sykim@koreatech.ac.kr; savaskaya@cumhuriyet.edu.tr
[1] Interaction Laboratory, Advanced Technology Research Center, Future Convergence Engineering, Korea University of Technology and Education (KoreaTech), Cheonan-si, Chungcheongnam-do 330-708, Republic of Korea
[3] Health Services Vocational School, Department of Pharmacy, Sivas Cumhuriyet University, Sivas 58140, Turkey
Full list of author information is available at the end of the article

Springer Open

© The Author(s) 2021. **Open Access** This article is licensed under a Creative Commons Attribution 4.0 International License, which permits use, sharing, adaptation, distribution and reproduction in any medium or format, as long as you give appropriate credit to the original author(s) and the source, provide a link to the Creative Commons licence, and indicate if changes were made. The images or other third party material in this article are included in the article's Creative Commons licence, unless indicated otherwise in a credit line to the material. If material is not included in the article's Creative Commons licence and your intended use is not permitted by statutory regulation or exceeds the permitted use, you will need to obtain permission directly from the copyright holder. To view a copy of this licence, visit http://creativecommons.org/licenses/by/4.0/.

anemia, leucopoenia and mental decentralization (Kingsley et al. 2015; D'Souza et al. 2017); also, the FA is very much important for the biosynthesis of catecholamines (Goldstein et al. 1966). The FA supplementation has significant effect on human health condition, and it can effectively protect against stroke (Huang et al. 2012). Pregnant women are advised to consume folic acid to prevent neural tube defects (NTDs) associated with congenital deformities of the spinal column, skull and brain of the fetus (Toriello 2005). NTDs play an adverse role in the cause of global mortality and morbidity with an estimated incidence of > 300,000 cases per year (Cordero et al. 2010a). To prevent NTDs caused by deficiency of FA, an intake of 0.2 mg/day for adults and 0.4 mg/day for pregnant woman was recommended by Centers for Disease Control and Prevention (Cordero et al. 2010b). FA is essential for fertility in men also, it contributes to spermatogenesis, and an appropriate quantity of FA can prevent subfertility in man (Azizollahi et al. 2013). Therefore, accurate and precise determination of FA in pharmaceutical samples, food products and in the human body is of great importance in medical and bioanalytical fields of research. Various methods were reported for the FA determination, including spectrophotometry (Nagaraja et al. 2002), chromatography (Young et al. 2011) and fluorescence (Giron et al. 2008). However, these methods suffer from severe drawbacks like complexity, expensive instrumentation, use of organic solvents and time consumption. Recently, the electroanalytical methods for FA determination have showed promising results with great accuracy, good reproducibility, selectivity and high sensitivity, simplicity and cost-effectiveness (Afshar et al. 2020; Kingsley et al. 2015; D'Souza et al. 2017; Yuan et al. 2020).

Over the past few decades, electrochemical sensors have been used as an effective sensing platform for the detection of heavy metals (Ye et al. 2020; Sultan et al. 2019), pharmaceutical and clinical samples (Ganesh et al. 2021a, 2021b), organic toxic pollutants (Ganesh et al. 2021c; Gowri and John et al. 2020), pesticides and herbicides (Prasad et al. 2019; Demir 2019) and neurotransmitters (Setoudeh et al. 2020). The carbon paste electrode (CPE) shows a promising applicability as an electrochemical sensor due to its wide potential window, low ohmic resistance, easy preparation, bulk surface modification and non-toxicity (Maleh et al. 2019). In order to enhance the sensing performance and to prevent the surface fouling of the CPE, a surface modification is the best strategy (Nunez et al. 2018). Several kinds of modification procedures have been reported recently (Afshar et al. 2020; Kingsley et al. 2015; D'Souza et al. 2017; Ganesh et al. 2021a, b, c; Gowri and John et al. 2020; Setoudeh et al. 2020). Among all these kinds of modification procedure, electropolymerization method is one of the easy and convenient way of modifying the carbon paste electrode (Ganesh et al. 2021a, b,c). The modified electrodes fabricated by electropolymerization method are simple and economic and showed a promising sensing capability. On the other hand, they exhibited high sensitivity, selectivity, reproducibility and antifouling property toward analyte determination. Niacin (nicotinic acid or pyridine 3-carboxylic acid) (see supplementary Fig.S1) is a simple organic compound, and it can be efficiently used to modify the carbon paste electrode due to its biocompatibility and simple structure. The acid and base dissociation constants for niacin are 2.79 and 4.19, respectively, corresponding to deprotonation of carboxylic acid and protonation of pyridine nitrogen. When niacin is dissolved in water, the carboxylic acid proton dissociates and the pyridine is protonated, forming the zwitterion (Lovander et al. 2018). Recently, there is a report on poly(niacin) based sensing electrode for the detection of caffeine and vanillin (Pushpanjali et al. 2020). The author Teradale et al. reported the application of niacin film-coated CPE toward the determination of epinephrine and uric acid (Teradale et al. 2017). Poly (niacin) coated graphite paste electrode was successfully applied for the detection of riboflavin (Manjunatha et al. 2020). The overlapped oxidation signals of dopamine and uric acid was resolved at niacin-modified CPE (Manjunatha et al. 2012). Alizadeh et al. showed a remarkable reduction signal for niacin at a CPE without any modification (Alizadeh et al. 2020). It is assumed that a thin layer of niacin coating on the surface of working electrode behaves like an electron transfer mediator which intern increases the sensing ability. However, all these previous reported works did not make any attempt to explain the redox reactive sites and mediating mechanism of niacin monomer (Pushpanjali et al. 2020; Teradale et al. 2017; Manjunatha et al. 2020, 2012), which is very curious and worthwhile to study. Furthermore, the advantages of CPE modified with niacin has generated a lot of research interest among electrochemical researchers, and, without any compromise, the biocompatibility of niacin warrants further in-depth studies. Due to this, there is an increasing demand for the fabrication of modified electrodes based on niacin monomer. In the present work, we demonstrated the fabrication of niacin-modified carbon paste electrode (NC/CPE) in the electroanalysis of FA in physiological pH by voltammetric methods. Recently, to explain the mediating mechanism of modifiers the density functional theory (DFT)-based quantum chemical modeling has been successfully used (Ganesh et al. 2021a, b; Chandrashekar et al. 2019) (Additional file 1).

Herein, we used DFT-based quantum chemical modeling to predict the redox reactive sites and mediating mechanism of niacin molecule. The nucleophilic and

electrophilic regions of niacin are identified using the HOMO and LUMO densities. The natural bond orbital (NBO) analysis was used to describe the donor–acceptor interactions, which were crucial in understanding the modifier–analyte relationship. The fabricated NC/CPE has been effectively applied as a new sensor for FA determination in pharmaceutical formulations. The modified carbon paste proposed in the present work can be used as a filler material in needles to recognize the concentration of FA in biological fluids by voltammetric methods. The materials used in the fabrication of NC/CPE are nontoxic and have no side effects on biological systems. The biocompatible behavior of NC/CPE permits in-vivo and/or in-vitro diagnosis of NTDs associated with the low concentration level of FA. The experimental data with the novel prediction on modifier mediating mechanism using DFT calculations lay a new platform for future studies in nano-sensors and diagnostic applications.

Methods

Chemicals and instrumentation

Folic acid (M_{wt}: 441.4 g/mol) (2.5×10^{-3} M), niacin (M_{wt}: 123.109 g/mol) (25×10^{-3} M), potassium ferrocyanide (M_{wt}: 368.34 g/mol) (25×10^{-3} M), potassium ferricyanide (M_{wt}: 329.24 g/mol) (25×10^{-3} M) and potassium chloride (M_{wt}: 74.55 g/mol) (1.0 M) were purchased from Sigma-Aldrich, Republic of Korea. The graphite powder and silicone oil (binder) were obtained from Sigma-Aldrich, Republic of Korea, respectively. Buffer solution (PBS, 0.2 M) of unique ionic strength and required pH was prepared by mixing respective volume of 0.2 M $NaH_2PO_4 \cdot H_2O$ and 0.2 M Na_2HPO_4 solution. We used double distilled water to prepare all the stock solutions. The reagents and chemicals mentioned are purely analytically graded, used as received without any purification. All electrochemical testings were carried out with electrochemical workstation (CHI660D). The electrolytic cell comprised three electrodes, namely reference (saturated calomel electrode, SCE), counter (platinum wire) and working electrode (bare or modified carbon paste electrode). All the potential values obtained were reported versus SCE at an ambient temperature.

Preparation of bare carbon paste electrode

The carbon paste was prepared by an add-mixing of finely ground graphite powder (70%) and binder (30%, silicon oil) in a mortar till a homogenous thick paste was obtained. This paste was then transferred and tightly packed into the cavity of the carbon paste electrode (CPE) and then smoothened on a piece of paper; later it was named as bare carbon paste electrode (bare/CPE) (Ganesh et al. 2021a).

Computational and theoretical study

The B3LYP (Becke 1993; Lee et al. 1988) and GD3BJ (Grimme 2006; Grimme et al. 2011) B3LYP functionals of the DFT were used to perform the geometry optimizations and frequency analyzes of the niacin, at 6-311G** (Krishnan et al. 1980; McLean and Chandler 1980) basis set. The QCP "quantum chemical parameters" were obtained from the FMO (frontier molecular orbital) analyses that were performed to get the ionization energy (I) and electron affinity (A) according to the Koopmans' Theorem (Koopmans 1934) given by the following equations

$$I = -E_{HOMO} \tag{1}$$

$$A = -E_{LUMO} \tag{2}$$

Besides, the C-DFT "conceptual density functional theory" (Parr & Pearson 1983; Pearson 1989; Parr et al. 1999; Islam & Kaya 2018) has defined the $\chi \rightarrow$ "electronic chemical potential," $\eta \rightarrow$ "global hardness," $\omega \rightarrow$ "electrophilicity", and $\Delta N_{max} \rightarrow$ "maximum charge transfer capability" indexes.

$$\chi = -\frac{I + A}{2} \tag{3}$$

$$\eta = \frac{I - A}{2} \tag{4}$$

$$\omega = \frac{\mu^2}{2\eta} \tag{5}$$

$$\Delta N_{max} = \frac{I + A}{2(I - A)} \tag{6}$$

Recently, the ω^- "the electro-donating power" and ω^+ "the electro-accepting power" values (Gazquez et al. 2007) are used to evaluate the specific reactivity properties and are defined as the following formulae.

$$\omega^+ \approx (I + 3A)^2/(16(I - A)) \tag{7}$$

$$\omega^- \approx (3I + A)^2/(16(I - A)) \tag{8}$$

The $\Delta E_{back\text{-}donation}$ "back-donation energy" (Gomez et al. 2006) is obtained from the equation below.

$$\Delta E_{back-donation} = -\frac{\eta}{4} \tag{9}$$

The NBO "natural bond orbital" analysis (Foster & Weinhold 1980; Reed et al. 1985a, b; 1988) has been used to elucidate the donor–acceptor interactions existing in a molecular system. In NBO analysis, the $E^{(2)}$ "lowering of

the stabilization energy" is calculated depending on the $q_i \rightarrow$ "bonding orbital occupancy," εi and εj → "bonding and antibonding orbital energies" (diagonal elements), and *Fij* → the off-diagonal NBO Fock matrix element.

$$E^{(2)} = \Delta E_{ij} = qi\frac{(Fij)^2}{(\varepsilon j - ?i)} \quad (10)$$

In all quantum chemical calculations, G09W (Frisch et al. 2013) and Gauss View 6.0.16 (GaussView 2016) packages were used.

Results and discussion

Fabrication of NC/CPE and its characterization

Many researchers have adopted cyclic voltammetric method to immobilize simple organic molecules on working electrodes by electropolymerization method (Ganesh et al. 2021a, b,c; Pushpanjali et al. 2020; Teradale et al. 2017; Manjunatha et al. 2020, 2012; Chandrashekar et al. 2019). In order to fabricate the NC/CPE, the following protocol was adopted; in an electrolytic cell, a solution of niacin monomer (1.0 mM) in PBS (0.2 M, pH 7.4) was sweeped between the potential of −0.8 to 1.8 V for consecutive 15 cycles with the scan rate of 0.1 Vs^{-1} as shown in Fig. S2. (see supplementary information). From Fig.S2, it can be observed that there is an increase in peak currents with an increasing number of sweep cycles; this suggests the initial growth of the polymer chain on the CPE. Later, after few successive cycles the voltammogram achieved a stable current response indicating the saturation level of electropolymerization (Ganesh et al. 2021a, b,c). It is well known that, with the greater number of cyclic sweeps the thickness of the polymer layer increases on CPE; as a consequence, a decrease in electrocatalytic property was observed as shown in Fig. S3 (see supplementary information). This might be due to the over thickness of polymeric film and less exposure of carbon paste surface (Ganesh et al. 2021a, 2021b; Ganesh et al. 2021a, b,c; Chandrashekar et al. 2019). Therefore, to achieve the remarkable voltammograms fifteen cyclic sweeps were considered to fabricate the NC/CPE.

An approximate estimation of surface coverage (Γ) was calculated by using Eq. (11) (Wang 1994; Sharp et al. 1979).

$$\mathrm{Ip} = \mathrm{n^2F^2A\Gamma\upsilon/4RT} \quad (11)$$

where n is number of electrons exchanged, A (cm^2), υ(V/s) and Ip (A) are the area of the working electrode, scan rate and peak current, respectively. The universal constants T (K), R (J K^{-1} mol^{-1}) and F (C mol^{-1}) have their usual significance. The Γ (mol/cm^2) was calculated to be 0.2102×10^{-10} mol/cm^2. In order to show the successful modification and to understand the surface texture of bare/CPE and NC/CPE, the scanning electron micrographs (SEM) were captured. It can be observed from Fig. 1(A-B) that the NC/CPE (B) comprises randomly aliened elevations and valleys as compared to the bare/CPE (A). As a result, in addition to the effect of the modifier's redox reactive sites, this special surface texture provided a route for NC/CPE to sense the analyte.

Figure 1C shows the cyclic voltammograms (CV) of 1 mM $Fe^{2+/3+}$ in 1.0 M KCl as a standard redox couple, at bare/CPE (curve a) and NC/CPE (curve c) with scan rate 0.05Vs^{-1}. We recorded blank CV (in the absence of $Fe^{2+/3+}$) at NC/CPE to confirm there is no interference by unreacted niacin monomer in the given potential range as shown in curve b of Fig. 1C. At bare/CPE, the oxidation peak potential (Epa) and reduction peak potential (Epc) of $Fe^{2+/3+}$ were located at 0.2772 V and 0.1806 V, respectively, with the peak potential difference (ΔEp) of 0.0966 V. This huge ΔEp is attributed to the sluggish electron transfer kinetics at bare electrodes (Ameur et al. 2013). However, after the modification the redox peak potentials corresponding to $Fe^{2+/3+}$ redox probe were observed at Epa = 0.2632 V and Epc = 0.1982 V, respectively, with the ΔEp = 0.0650 V. And also, the ratio of anodic peak current (Ipa) and cathodic peak current (Ipc) was found to be 1.16 (≈1.0), signifying the reversible process at NC/CPE. The electroactive surface area (EASA) of the working electrode was calculated by using the Randles–Sevcik's formulae (Ganesh et al. 2021a). The effect of number of cyclic sweeps on the fabrication of NC/CPE and corresponding EASA was calculated and is given in Table S1 (see supplementary file). As expected, the NC/CPE fabricated with 15 cyclic sweeps showed higher EASA (0.3762 cm^2) as compared to BCPE (0.2798 cm^2). Therefore, the modification of carbon paste electrode through electropolymerization of biocompatible niacin molecule increased the number of redox reactive sites that can be reflected in higher surface area of modified electrode with the advantages of minimization in the over potential.

Physicochemical and quantum chemical studies

Thermodynamic quantities provide very useful information on a specific reaction and/or interaction process between the reactant(s) and product(s) and are generally determined experimentally. On the other hand, these quantities are also successfully predicted theoretically (Serdaroğlu 2011) depending on the development of both the computer and technological sciences. The optimized geometries and physical quantities of two niacin conformers are displayed in Table 1 and Fig. 2, respectively. For both functional, the dipole moment of the N2 structure was calculated lower than the N1 conformer. Except for the dipole moments, all physicochemical quantities

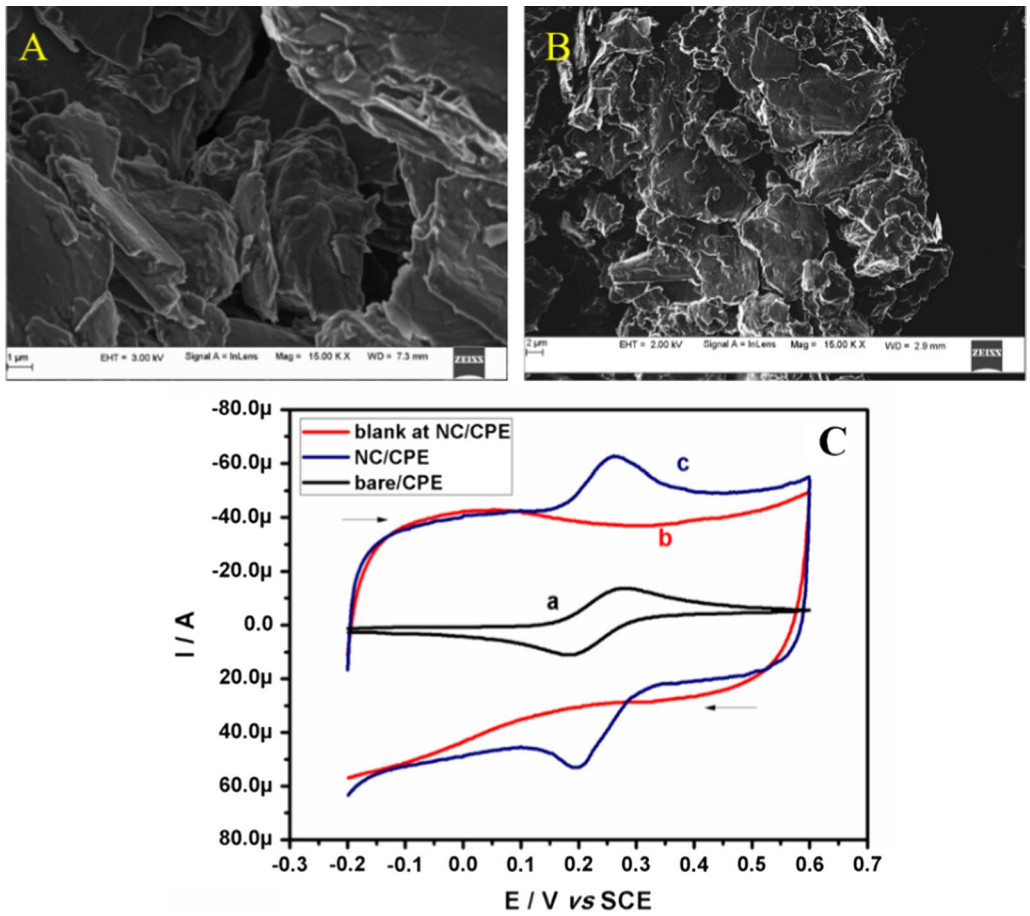

Fig. 1 Scanning electron micrograph images for bare/CPE **(A)** and NC/CPE **(B)**. **(C)** CVs for the 1 mM of $Fe^{2+/3+}$ in 1 M KCl as a supporting electrolyte at bare/CPE (curve a) and NC/CPE (curve c), the curve b represents the voltammogram in absence of analyte at NC/CPE; at scan rate of 0.05 Vs^{-1}

Table 1 The calculated physiochemical quantities of the niacin at B3LYP/6-311G** level

	B3LYP		B3LYP-GD3BJ	
	N1	N2	N1	N2
DM (debye)	3.246	0.569	3.248	0.566
α (au)	72.360	72.288	72.293	72.221
ΔE (au)	− 436.872568	− 436.872920	− 436.897002	− 436.897358
ΔH (au)	− 436.864611	− 436.864968	− 436.889043	− 436.889403
ΔG (au)	− 436.904559	− 436.904900	− 436.929011	− 436.929352
$\Delta E_{thermal}$ (kcal/mol)	69.406	69.417	69.459	69.469
Cv (cal/molK)	26.317	26.300	26.301	26.284
S (cal/molK)	84.079	84.044	84.120	84.080

were found very close to each other by both functionals. The polarizability values of N1 and N2 structures of the niacin were calculated as 72.360 au and 72.288 au at B3LYP, and 72.293 au and 72.221 au at GD3BJ functional, respectively. However, it should be said that the N2 structure was more stable thermodynamically than the N1 structure as the ΔG values of N1 and N2 were calculated at -436.904559 au and -436.904900 au, respectively.

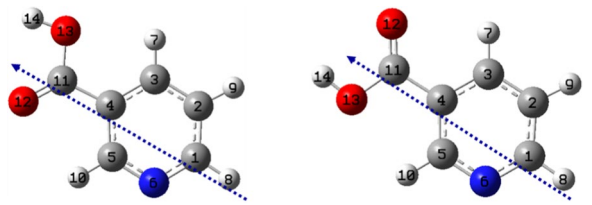

N1 **N2**

Fig. 2 The optimized structures of two conformers (N1 and N2) of the Niacin at B3LYP/6-311G** level

Also, the $\Delta E_{thermal}$ value of the N2 (69.417 kcal/mol) was also calculated as greater than the N1 (69.406 kcal/mol), at B3LYP. Based on the absolute entropy values, the N1 (84.079 cal/molK) structure was slightly more random than the N2 (84.044 cal/molK), at the B3LYP level.

Natural bond orbital study

In recent years, the donor–acceptor interactions based on the NBO theory have been also used to elucidate the chemical reactivity trend in a wide group of the compound (Mary et al. 2021; Serdaroğlu 2020). For both conformers, the second-order perturbative energy analysis results are summarized in Table 2. It should be noticed from Table 2 that the number and energies of the interactions between the filled and unfilled molecular orbitals were calculated similar to each other, even though the orbitals where electron transfer took place were different from each other, especially at the aromatic ring. Besides, the biggest contribution to the $E^{(2)}$ for both structures was sourced from the charge delocalization over the carboxylic group of the niacin. Namely, the highest energy interaction for N1 and N2 structures was determined as LP (2) O13 → Π* C11-O12 with $E^{(2)}$ of 43.58 kcal/ mol and 43.24 kcal/ mol, respectively. The $E^{(2)}$ value of the LP (2) O12 ($ED_i = 1.84498e$) → σ* C4-C11 ($ED_j = 0.06812e$) interaction for N1 structures was calculated as 18.23 kcal/mol that was almost similar to that of N2 structure. Also, the energy of the LP (1) N6 → σ* C4-C5 interaction was estimated at 9.79 kcal/ mol for N1 and 9.86 kcal/mol for N2, respectively. Besides, the energy of the Π C11-O12 → Π* C3-N4 interaction for N1 and N2 was determined in 4.27 kcal/mol and 4.21 kcal/mol, respectively, even though they did not contribute significantly to $E^{(2)}$. The significant contribution to $E^{(2)}$ for N1 structure came from the Π C3-C4

Table 2 NBO analysis results of two conformers (N1 and N2) of Niacin at B3LYP/6-311G** level

Donor(i)	ED_i/e	Acceptor (j)	ED_j/e	$E^{(2)}$/ kcalmol^{-1}	E(j)-E(i)/ a.u	F(i.j)/ a.u
N1						
Π C1-C2	1.61973	Π* C3-C4	0.35251	25.33	0.28	0.076
		Π* C5-N6	0.33157	15.45	0.27	0.059
Π C3-C4	1.62896	Π* C1-C2	0.29389	15.91	0.28	0.061
		Π* C5-N6	0.33157	28.38	0.27	0.08
		Π* C11-O12	0.24265	21.48	0.27	0.071
Π C5-N6	1.70191	Π* C1-C2	0.29389	27.95	0.32	0.084
		Π* C3-N4	0.35251	12.97	0.32	0.058
Π C11-O12	1.98358	Π* C3-N4	0.35251	4.27	0.41	0.041
LP (2) O12	1.84498	σ* C4-C11	0.06812	18.23	0.68	0.102
LP (2) O13	1.82621	Π* C11-O12	0.24265	43.58	0.35	0.112
LP (1) N6	1.91913	σ* C4-C5	0.03309	9.79	0.89	0.084
N2						
Π C1-N6	1.69677	Π* C2-C3	0.27915	12.65	0.32	0.057
		Π* C4-C5	0.33577	28.72	0.32	0.086
Π C2-C3	1.63728	Π* C1-N6	0.36346	29.9	0.27	0.08
		Π* C4-N5	0.33577	16.97	0.28	0.062
Π C4-N5	1.61608	Π* C1-N6	0.36346	15.69	0.27	0.058
		Π* C2-C3	0.27915	23.09	0.29	0.075
		Π* C11-O12	0.24458	21.87	0.27	0.071
Π C11-O12	1.9839	Π* C4-C5	0.33577	4.21	0.41	0.04
LP (2) O12	1.84618	σ* C4-C11	0.06856	18.22	0.68	0.102
LP (2) O13	1.82387	Π* C11-O12	0.24458	43.24	0.35	0.112
LP (1) N6	1.91901	σ* C4-C5	0.33577	9.86	0.89	0.084

($ED_i = 1.62896e$) → Π* C5-N6 ($ED_j = 0.33157e$) interaction with the energy of 28.38 kcal/ mol. Instead of, Π C2-C3 ($ED_i = 1.63728e$) → Π* C1-N6 ($ED_j = 0.36346e$) interaction for N2 structure contributed to significantly to $E^{(2)}$ (29.90 kcal/mol) that was almost similar energetically to N2 structure.

Global reactivity study

The quantum chemical parameters (QCP) is widely used to estimate the chemical tendency of both the basic (Jacob et al. 2020) and complex molecular systems (Serdaroğlu et al. 2021). Table 3 illustrates the calculated QCP for N1 and N2 structures of the niacin. In general, the results obtained from the B3LYP level and their tendencies of them were almost similar to the GD3BJ level. The E_{HOMO} (H), E_{LUMO} (L), and ΔE_{gap} (L–H) values were calculated by B3LYP level as −7.358, −1.908, and 5.450 eV for N1 and −7.362, −1.900, and 5.461 eV for N2, respectively. Besides, the μ, η, ΔN_{max} values of N1 were predicted in -4.633, 2.725, and 1.700 eV, whereas these values for N2 were estimated as -4.631, 2.731, and 1.696 eV, respectively, at B3LYP. For N1 and N2 structures, ω index was calculated in 3.939 eV and 3.927 eV by B3LYP and 3.935 eV and 3.925 eV by GD3BJ level. In any case, the electro-donating power of both N1 and N2 structures was dominant over electro-accepting potency. Namely, the ω^+ and ω^- indexes for both structures were determined by B3LYP functional as 0.072 au and 0.242 au, respectively. Similarly, the $\Delta\varepsilon_{back\text{-}donat.}$ (eV) value for N1 and N2 was estimated as −0.681 eV and −0.683 eV, respectively, which implied that the back donation for each structure was favorable energetically.

The pictorial representation of the reactive region of N1 and N2 structures is given in Fig. 3. As known well, the illustrations of the HOMO and LUMO densities are used to indicate the nucleophilic and electrophilic regions of any chemical species. Accordingly, the HOMO density covered up the pyridine ring and partly on the oxygen atoms of the carboxylic group. However, the LUMO spread over the whole molecular surface for both N1 and N2 structures, excluding the several H atoms. In addition, the MEP graphs for both structures indicated the electron-rich site was around the oxygen of C=O group that seem by red color as a function of the electrostatic potential. Also, the N atom on the pyridine ring was surrounded by yellow color as a sign of the moderate negative electrostatic potential. Furthermore, the blue color as a marker of the positive electrostatic potential densified on the H atom of the -OH group was the best site for the nucleophilic attack.

Table 3 The quantum chemical parameters of two conformers (N1 and N2) of Niacin at B3LYP/6-311G** level

	N1	N2	N1	N2
H (-I) (eV)	− 7.358	− 7.362	− 7.356	− 7.360
L (-A) (eV)	− 1.908	− 1.900	− 1.906	− 1.899
ΔE (L–H) (eV)	5.450	5.461	5.450	5.461
μ (eV)	− 4.633	− 4.631	− 4.631	− 4.629
η (eV)	2.725	2.731	2.725	2.730
ω (eV)	3.939	3.927	3.935	3.925
ω^+ (au)	0.072	0.072	0.072	0.072
ω^- (au)	0.242	0.242	0.242	0.242
$\Delta\varepsilon_{back\text{-}donat.}$ (eV)	− 0.681	− 0.683	− 0.681	− 0.683
ΔN_{max} (eV)	1.700	1.696	1.700	1.696

Electrochemical behavior of FA at NC/CPE

To study the electrochemical behavior of FA at bare/CPE (curve a) and NC/CPE (curve c), cyclic voltammetry was used; the curve c represents the blank voltammogram (in the absence of FA) at NC/CPE. Figure 4 shows the CVs of 40.0 μM FA in PBS (0.2 M, pH 7.4) at scan rate $0.05 Vs^{-1}$. As can be seen from Fig. 4, there is no prominent peak for the oxidation of FA at bare/CPE, while at NC/CPE a well-defined oxidation peak of FA was observed. FA showed the oxidation potentials at 0.6947 V and 0.6464 V for bare/CPE and NC/CPE, respectively. The Ipa of FA at bare/CPE and NC/CPE was 2.229 μA and 20.721 μA, respectively. A shift toward a lower oxidation potential and ten times increment in oxidative current at NC/CPE provide evidence for the charge transfer reaction at NC/CPE toward the electrocatalytic oxidation of FA.

The influence of varying scan rate (0.020—0.26 Vs^{-1}) was studied using 10.0 μM FA in PBS (0.2 M, pH 7.4) at NC/CPE by CV method, as shown in Fig. 5A. The Ipa was found to be proportional to the corresponding applied scan rate with correlation coefficient $r^2 = 0.9965$ as shown in Fig. 5B, with linear regression equation Ipa (μA) = 0.0809 υ (mVs^{-1}) + 2.5897 suggesting the adsorption dominated electrode process (D'Souza et al. 2017). On the other hand, the linear establishment between logarithm of scan rate (logυ) with logarithm of peak current (log Ipa) gives a slope of 0.7202 as shown in Fig. 5C; this confirms the electrode reaction of FA at NC/CPE is meticulously controlled by adsorption kinetics (Kingsley et al. 2015; D'Souza et al. 2017). A linear graph of Epa versus log υ is presented in Fig. 5D, which shows a linear regression equation as follows:

$$\mathrm{Epa(mV)} = 65.158 \log \upsilon (\mathrm{mVs^{-1}}) + 543.33 (r^2 = 0.9858)$$

As suggested by Laviron's Eq. (12) (Jiang et al. 2013), for an irreversible electrode process the Epa can be defined as follows:

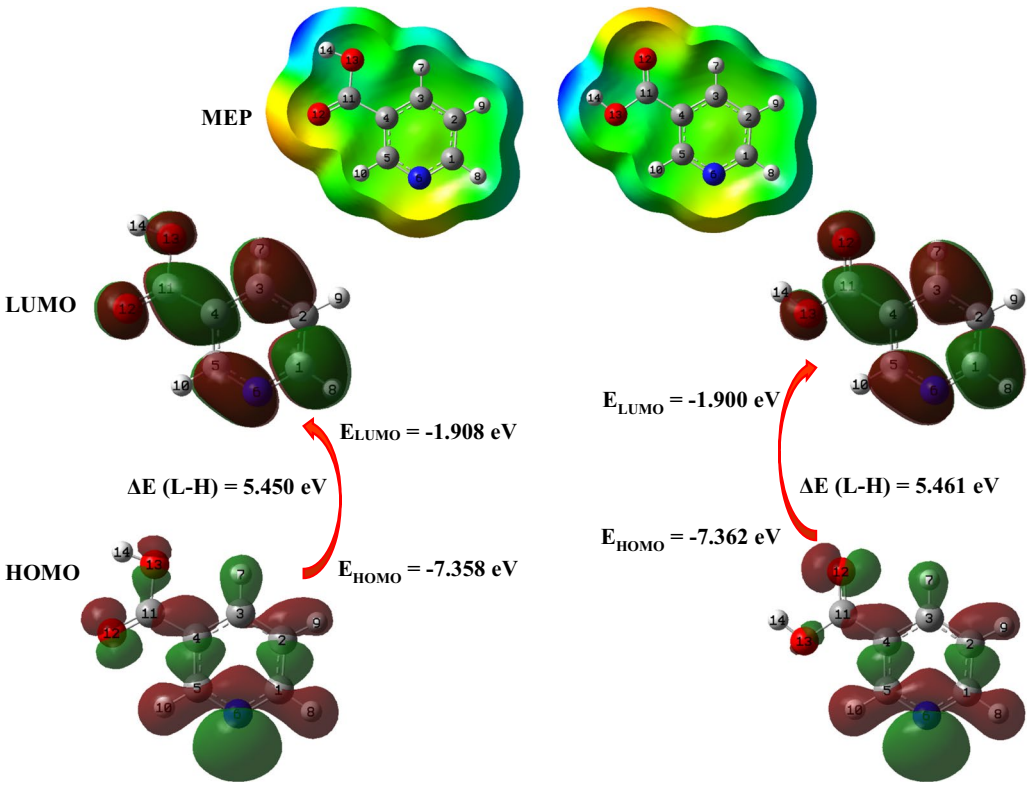

Fig. 3 HOMO and LUMO (isoval: 0.02), and MEP (isoval: 0.0004) pilots of two conformers (N1 and N2) of Niacin at B3LYP/6-311G** level

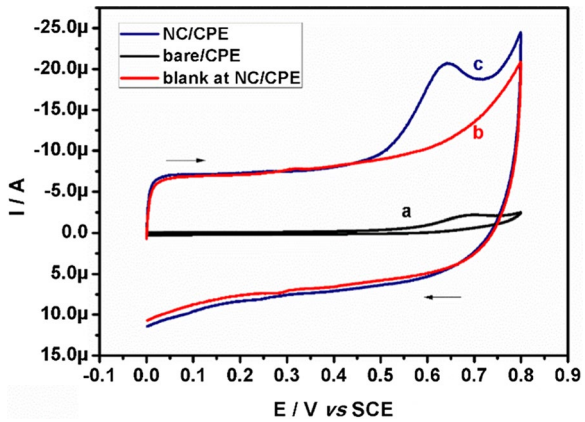

Fig. 4 CVs of 40.0 µM FA in 0.2 M PBS (pH 7.4) at bare/CPE (curve a) and NC/CPE (curve c), the curve b represents the voltammogram in absence of FA at NC/CPE; at the scan rate of 0.05 Vs^{-1}

$$Epa = \left[\frac{2.303RT}{2(1-\alpha)nF}\right] \log \upsilon + K \quad (12)$$

where α and n are the charge transfer coefficients and number of electrons involved, respectively. R, T and F are constants with their usual significance. In Eq. (12), the term 2.303RT/2(1-α) nF represents the slope of linear plot in Fig. 5D. For an irreversible electrode process, α is 0.5 (D'Souza et al. 2017); the n value was calculated to be 1.78, which agrees with the previous report (Wei et al. 2006). We also calculated the standard heterogeneous rate constant (k^0) by referring the previous literature (Gowda et al. 2017). The k^0 can be determined from the intercept of Ep versus logυ, if the value of E^0 is known. The value of E^0 can be obtained from the intercept of Epa versus υ by extrapolating to the vertical axis at υ = 0. The value of k^0 was calculated to be 9.21×10^3 s^{-1}.

Effect of solution pH

The influence of solution pH on Epa and Ipa of 30.0 µM FA in 0.2 M PBS of different pH was studied by CV at NC/CPE, with scan rate 0.05 Vs^{-1}. Figure 6A shows the CVs of FA at NC/CPE in the pH range 5.5 to 8.0. The NC/CPE exhibited pH-dependent sensitivity for FA; at pH 6.0, the Ipa of FA was found to maximum due to the instability of FA in acidic conditions (D'Souza et al. 2017). The Epa of FA was slightly shifted toward negative potential scale with the increasing pH, signifying the involvement of protons in the electrooxidation of FA. The relationship between Epa and pH is shown in Fig. 6B, which gives a linear regression equation: Epa (V) = 0.7884–0.0289 pH (r^2 = 0.9218).

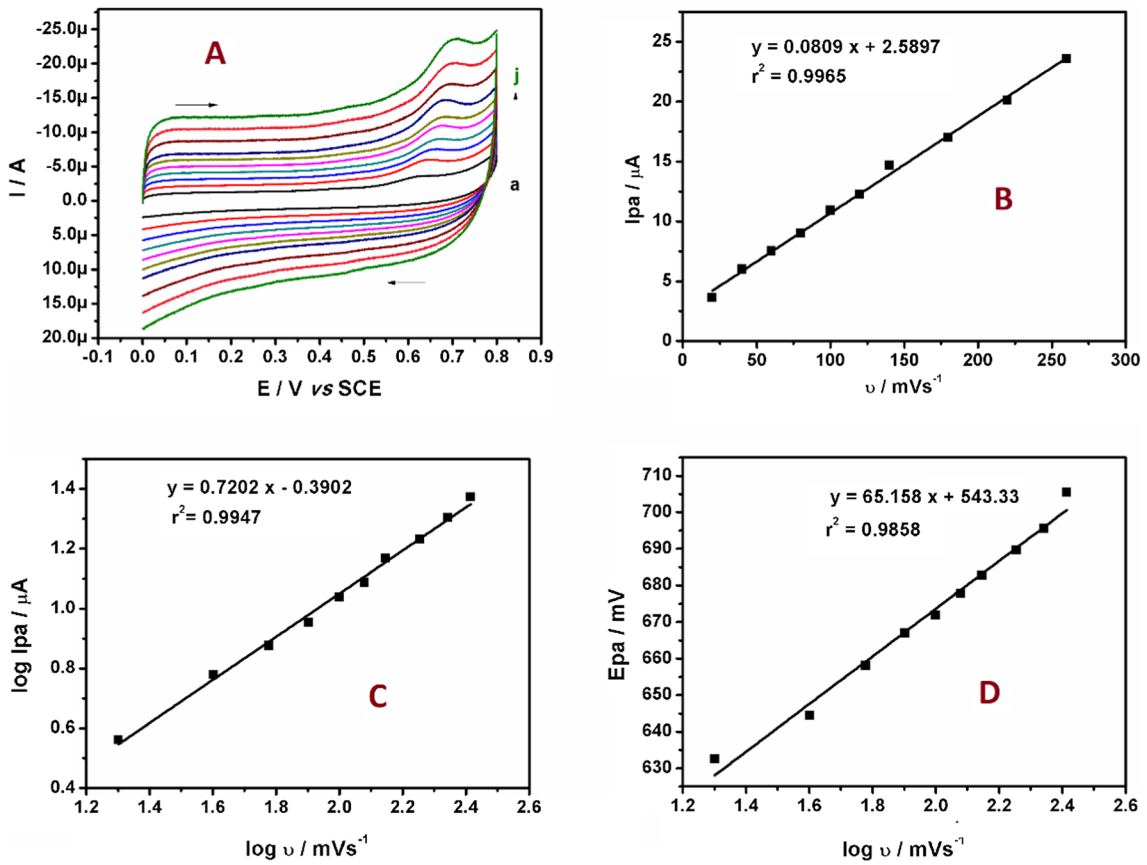

Fig. 5 **A** CVs of 10.0 µM FA at NC/CPE with varying scan rates (a–j; 0.020 Vs^{-1} to 0.260 Vs^{-1}) in 0.2 M PBS (pH 7.4). **B** Graph of Ipa versus υ. **C** Graph of log Ipa versus log υ. **D** Graph of Epa versus log υ

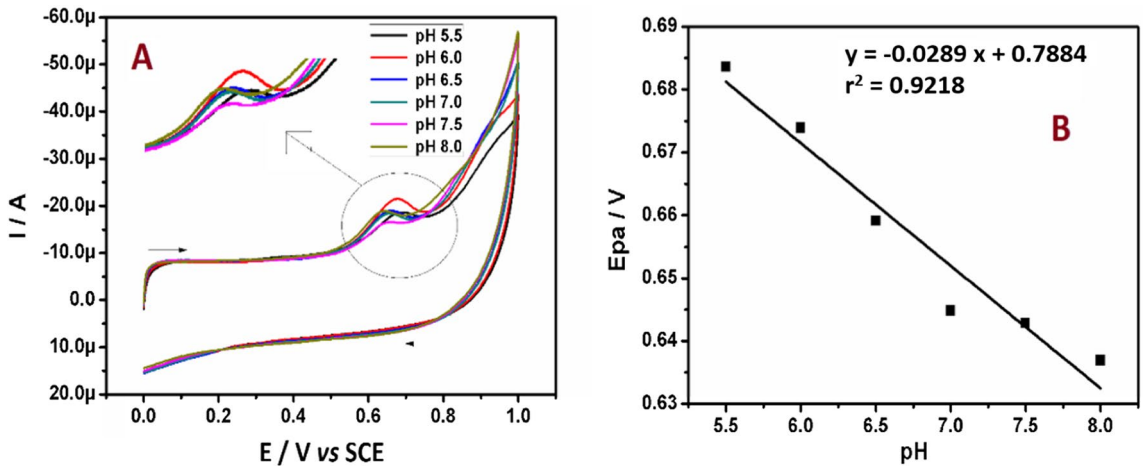

Fig. 6 **A** CVs of 30.0 µM FA at NC/CPE in 0.2 M PBS of different pH (5.5 to 8.0) with the scan rate of 0.05Vs^{-1}. **B** The effect of pH on anodic peak potential

The slope of Epa versus pH was—0.0289. This suggests the electrooxidation of FA at NC/CPE involves transfer to two electrons and one proton (D'Souza et al. 2017). This result agreed with previous report (Nie et al. 2013; D'Souza et al. 2017).

Effect of FA concentration NC/CPE

Figure 7A shows the CVs recorded for the different concentrations of FA at NC/CPE, with the applied scan rate of $0.05Vs^{-1}$. It can be seen from Fig. 7A that the Ipa of FA enhanced with its increasing concentration in the range 5.0 µM to 45.0 µM. The liner plot of Ipa versus concentration of FA yields a linear regression equation, Ipa (µA) = 0.0197 C_0 µM/L + 1.2329 (r^2 = 0.9897) as shown in Fig. 7B. The limit of detection (LOD) and limit of quantification (LOQ) were calculated by using Eqs. (13) and (14), respectively.

$$\mathrm{LOD} = 3\ \mathrm{s/m} \tag{13}$$

$$\mathrm{LOQ} = 10\ \mathrm{s/m} \tag{14}$$

where s is the standard deviation of six blank measurements and m is slope of the calibration graph (Ganesh et al. 2021b; Analytical Methods Committee 1987). The LOD and LOQ of FA at NC/CPE was calculated to be 0.09 µM and 0.3 µM, respectively; this was comparatively lower as compared to previous reports as given in Table 4 (Afshar et al. 2020; Yuan et al. 2020; Ganesh et al. 2021a; Zhang et al. 2016; Kumara et al. 2019; Tanuja et al 2017; Narayana et al. 2015; Ojani et al. 2009; Garcia et al. 2021).

Effect of interferents

It is well known that some of the easily oxidizable species usually coexist with bio-samples and it may negatively impact on the detection of FA in real sample analysis. Therefore, assessing the selectivity and anti-interference property of NC/CPE plays a significant role to be consider it for real sample analysis (Ashrafi et al. 2014). The

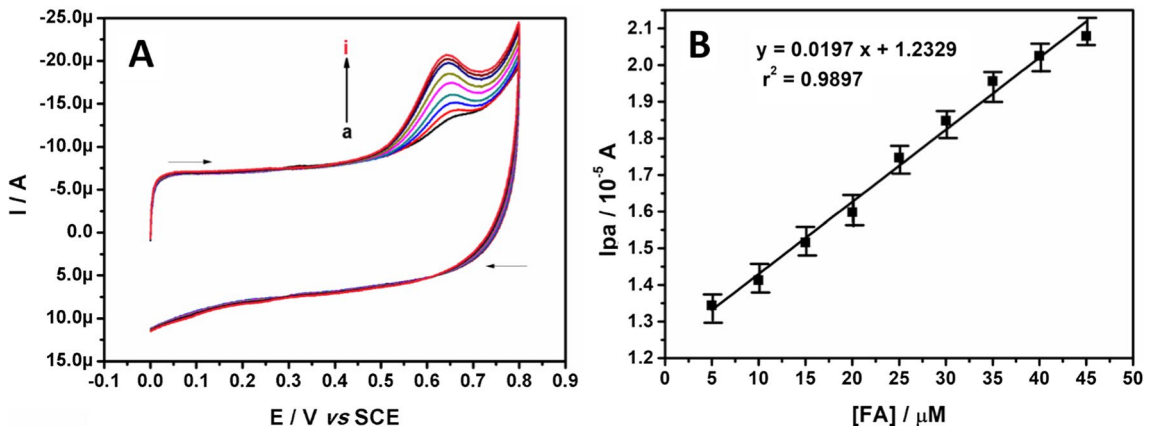

Fig. 7 **A** Cyclic voltammograms of FA in 0.2 M PBS (pH 7.4) at NC/CPE at scan rate of $0.05Vs^{-1}$ with different concentration (a-i; 5.0 µM to 45.0 µM). **B** Graph of anodic peak current versus concentration of FA

Table 4 Comparison of LOD obtained at NC/CPE for FA with other recently reported modified electrodes

Sl no	Working electrode	LOD ((µM)	Concentration range (µM)	pH	method	Reference
1	NiO/SWCNTs/1B3MIMS/CPE	0.07	0.3–350	7.0	DPV	Afshar et al. (2020)
2	PtNPs-GNPs-MWCNTs-β-CD/GCE	0.48	20.0–500.0	7.0	CV	Yuan et al. (2020)
3	BRB/CPE	1.04	106.0–142.0	7.4	CV	Ganesh et al. (2021a)
4	MB/ERGO/GCE	0.5	4.0–167	7.4	DPV	Zhang et al. (2016)
5	ZnO/FMWCNT MCPE	1.3	5.0–20.0	7.4	CV	Kumara et al. (2019)
6	Nevirapine-modified CPE	2.5	5.0–45.0	7.0	DPV	Tanuja et al 2017
7	poly(ser)/MWCNTs/GCE	0.6	5.0–110.0	7.0	DPV	Narayana et al. (2015)
8	Ni-poly(o-anisidine)/CPE	91.0	100–5000	2.0	CV	Ojani et al. (2009)
9	Fe_3O_4@MIP-GO/CPE	0.65	2.5–48.0	7.0	SWV	Garcia et al. (2021)
10	NC/CPE	0.09	5.0–45.0	7.4	CV	This work

impact of various coexisting interferents on the voltammogram of 30.0 μM FA was investigated and is shown in Table S2 (see supplementary file). The excipients like ascorbic acid, citric acid, dopamine, oxalic acid, uric acid, glucose, sucrose, lactose, glycine, catechol, hydroquinone, sodium chloride, ammonium chloride and calcium sulfate are added tenfold excess in the determination of FA at NC/CPE in order to evaluate the selectivity of the performance of the NC/CPE. The result indicated the current signal changed slightly but not exceeded 5.0%, which clearly justifies that the NC/CPE is a suitable sensing platform for FA and which is not affected by the existence of co-interferences.

Analytical application of NC/CPE in real samples and pharmaceuticals

The practical applicability of NC/CPE was evaluated by employing it to the analysis of FA in fruit juice and pharmaceutical sample using the standard addition method by CV technique. As reported by D'Souza et al., we extracted the juices of orange, lemon and tomato by finely blending; later, the blended liquid pulp was filtered through ordinary grade filter paper followed by filtration through Whatman paper (D'Souza et al. 2017). The clear filtrate was diluted with 0.2 M PBS of pH 7.4. We followed the standard addition method, and different concentrations of FA were added to the mentioned juice samples. Good recovery results were obtained at NC/CPE as shown in Table S3 (see supplementary file). The tablets containing FA were bought from a pharmacy and directly analyzed by CV technique followed by the sample preparation procedure as recently explained in the literature (Hanabaratti et al. 2020; Selcuk et al. 2021). The tablets were weighed and crushed into a fine powder using a mortar and pestle, and an adequate quantity of this sample was dissolved with double-distilled water and sonicated for 30 min to ensure complete dissolution. Later, the solution was filtered to remove undissolved solids; the obtained supernatant solution was diluted with 0.2 M PBS of pH 7.4. The standard addition method was used for recovery studies. Table S4 (see supplementary file) shows the results of the tablet analysis at NC/CPE. Overall, the results obtained at NC/CPE for real sample analysis were acceptable and it reflects the fabricated biocompatible NC/CPE can be successfully applied for the analytical assay of FA in biological samples without any interferences.

Conclusions

To enhance the analytical performance of the bare working electrode, the modification is the best and widely acceptable strategy. However, studying the modified electrode–analyte interaction is crucial to reveal the sensing mechanism and to fabricate an electrochemical sensor. In this regard, we used density functional theory (DFT)-based quantum chemical modeling to explore the sensing performance of the niacin-modified carbon paste electrode (NC/CPE). The natural bond orbital (NBO) results for optimized geometries of two niacin conformers structures disclosed that the resonance interactions were mainly responsible for the lowering of the stabilization energy. The FMO studies demonstrated that mainly the oxygen atom of the carboxyl group and partially the N atom were the best places for the electrophilic attack, and the H atom of the -OH group was determined as the best suitable site for the nucleophilic attacks. On the other hand, the limit of detection (LOD) for folic acid (FA) at NC/CPE was calculated to be 0.09 μM in the linear range of 5.0 μM to 45.0 μM. The performance of the NC/CPE in assessing FA in real samples, such as fruit juice and tablet samples, has been demonstrated to be satisfactory. Therefore, the modified electrode can be used for the analysis of electroactive molecules in pharmaceutical formulations. The methods used in this study can be applied to other electroactive compounds as well.

Abbreviations

FA: Folic acid; CPE: Carbon paste electrode; NC/CPE: Niacin-modified carbon paste electrode; NBO: Natural bond orbital; CV: Cyclic voltammetry; NTDs: Neural tube defects; DFT: Density functional theory; PBS: Phosphate buffer solution; SCE: Saturated calomel electrode; bare/CPE: Bare carbon paste electrode; QCP: Quantum chemical parameters; FMO: Frontier molecular orbital; Epa: Oxidation peak potential; Epc: Reduction peak potential; ΔEp: Peak potential difference; Ipa: Anodic peak current; Ipc: Cathodic peak current; EASA: Electroactive surface area; SEM: Scanning electron micrograph; logu: Logarithm of scan rate; log Ipa: Logarithm of peak current; k^0: Standard heterogeneous rate constant; LOD: Limit of detection.

Supplementary Information

The online version contains supplementary material available at https://doi.org/10.1186/s40543-021-00301-6.

Additional file 1. Figure S1. Niacin molecule. **Figure S2.** CVs during the fabrication of NC/CPE, an electrochemical cell containing 1.0 mM niacin monomer in 0.2 M PBS (pH 7.4) solution at 15 multiple cycles with the scan rate of 0.1 Vs^{-1}. **Figure S3.** Graph of anodic peak current versus number of polymerization cycles. **Table S1.** Effect of number of cyclic sweeps on the fabrication of NC/CPE and corresponding area of the modified electrode. **Table S2.** Influence of coexisting interferents on the voltammetric response of FA at NC/CPE. **Table S3.** Determination of FA in the juices of orange, lemon and tomato sample using NC/CPE (n = 3). **Table S4.** Determination of FA in the tablet sample using NC/CPE (n = 3).

Acknowledgements

The authors acknowledge Cooperative Equipment Center at KoreaTech for technical discussions and research facilities.

Authors' contributions

P.S.G. contributed to the conceptualization, visualization, experimental idea and writing of the manuscript; E.J.S. and S.H.L. were involved in the literature collection; P.S.G., D.S.C. and G.S[1] contributed to the methodology. P.S.G. contributed to the electrode fabrication and electrochemical experiments; S.K.,

G.S[4] and P.S.G. contributed to the computational studies; P.S.G. contributed to the writing—original draft; S.Y.K. contributed to the writing—review and editing; S.Y.K. contributed to the supervision; all authors discussed the results and agreed to the final version of the manuscript.

Funding
This work was supported by the National Research Foundation of Korea (NRF) grant funded by Ministry of Education (NRF-2020R1I1A3065371). This work was also supported by the Technology Innovation Program (10077367, Development of a film-type transparent/stretchable 3D touch sensor/haptic actuator combined module and advanced UI/UX) funded by the Ministry of Trade, Industry & Energy (MOTIE, Korea). This work was also supported by Institute of Information & Communications Technology Planning & Evaluation (IITP) grant funded by the Korea Government (MSIT) (No. 2020–0-00594, Morphable Haptic Controller for Manipulating VR·AR Contents).

Availability of data and materials
Not applicable.

Declarations

Competing interests
The authors declare that they have no competing interests.

Author details
[1]Interaction Laboratory, Advanced Technology Research Center, Future Convergence Engineering, Korea University of Technology and Education (KoreaTech), Cheonan-si, Chungcheongnam-do 330-708, Republic of Korea. [2]School of Computer Science, College of Engineering and Information Technology, Semyung University, Jecheon 27136, Chungcheongbuk-do, Republic of Korea. [3]Health Services Vocational School, Department of Pharmacy, Sivas Cumhuriyet University, Sivas 58140, Turkey. [4]Faculty of Education, Math. and Sci. Edu, Sivas Cumhuriyet University, 58140 Sivas, Turkey.

Received: 26 August 2021 Accepted: 14 October 2021
Published online: 22 October 2021

References

Afshar S, Zamani HA, Maleh HK. NiO/SWCNTs coupled with an ionic liquid composite for amplified carbon paste electrode; A feasible approach for improving sensing ability of adrenalone and folic acid in dosage form. J Pharm Biomed Anal. 2020;188: 113393. https://doi.org/10.1016/j.jpba.2020.113393.

Alizadeh T, Amjadi S. Determination of nicotinic acid by square wave voltammetry on a carbon paste electrode: the crucial effect of electrode composition and analytical conditions. Anal Bioanal Electrochem. 2020;12(2):250–62.

Ameur ZO, Husein MM. Electrochemical behavior of potassium ferricyanide in aqueous and (w/o) microemulsion systems in the presence of dispersed nickel nanoparticles. Sep Sci Technol. 2013;48(5):681–9. https://doi.org/10.1080/01496395.2012.712594.

Analytical Methods Committee. Recommendations for the definition. Estim Use Detect Limit. 1987;112:199–204. https://doi.org/10.1039/AN9871200199.

Ashrafi AM, Kurbanoglu S, Vytřas K, Uslu B, Ozkan SA. Electrochemical mechanism and sensitive assay of antiretroviral drug Abacavir in biological sample using multiwalled carbon nanotube modified pyrolytic graphite electrode. J Electroanal Chem. 2014;712:178–84. https://doi.org/10.1016/j.jelechem.2013.11.012.

Azizollahi G, Azizollahi S, Babaei H, Kianinejad M, Baneshi MR, Nematollahi-mahani SN. Effects of supplement therapy on sperm parameters, protamine content and acrosomal integrity of varicocelectomized subjects. J Assist Reprod Gen. 2013;30:593–9. https://doi.org/10.1007/s10815-013-9961-9.

Becke AD. Density-functional thermochemistry. III. The role of exact exchange, J Chem Phys. 1993;98;5648–5652. https://doi.org/10.1063/1.464913

Chandrashekar BN, Lv W, Jayaprakash GK, Harrath K, Liu LWY, Swamy BEK. Cyclic voltammetric and quantum chemical studies of a poly(methionine) modified carbon paste electrode for simultaneous detection of dopamine and uric acid. Chemosensors. 2019;7(2):24. https://doi.org/10.3390/chemosensors7020024.

Cordero A, Mulinare J, Berry RJ, Boyle C, Dietz W, Johnston R Jr, Leighton J, Popovic T. CDC grand rounds: additional opportunities to prevent neural tube defects with folic acid fortification. MMWR Morb Mortal Wkly Rep. 2010;59(31):980–4.

Cordero A, Mulinare J, Berry RJ, Boyle C, Dietz W, Johnston Jr R, Popovic T, CDC Grand rounds: additional opportunities to prevent neural tube defects with folic acid fortification. Morbidity and Mortality Weekly Report.2010b;59(31);973–979.

D'Souza OJ, Mascarenhas RJ, Satpati AK, Detriche S, Mekhalif Z, Delhalle J, Dhason A. High electrocatalytic oxidation of folic acid at carbon paste electrode bulk modified with iron nanoparticle-decorated multiwalled carbon nanotubes and its application in food and pharmaceutical analysis. Ionics. 2017;23:201–12. https://doi.org/10.1007/s11581-016-1806-y.

Demir E. A simple and sensitive square wave stripping pathway for the analysis of desmedipham herbicide by modified carbon paste electrode based on hematite (α-Fe_2O_3 nanoparticles). Electroanalysis. 2019;31(8):1545–53. https://doi.org/10.1002/elan.201800861.

Foster JP, Weinhold F. Natural hybrid orbitals. J Am Chem Soc. 1980;102(24):7211–8. https://doi.org/10.1021/ja00544a007.

Frisch MJ, Trucks GW, Schlegel HB, Scuseria GE, Robb MA, Cheeseman JR, Scalmani G, Barone V, Mennucci B, Petersson GA, Nakatsuji H, Caricato M, Li X, Hratchian HP, Izmaylov AF, Bloino J, Zheng G, Sonnenberg JL, Hada M, Ehara M, Toyota K, Fukuda R, Hasegawa J, Ishida M, Nakajima T, Honda Y, Kitao O, Nakai H, Vreven T, Montgomery Jr JA, Peralta JE, Ogliaro F, Bearpark M, Heyd JJ, Brothers E, Kudin KN, Staroverov VN, Keith T, Kobayashi R, Normand J, Raghavachari K, Rendell A, Burant JC, Iyengar SS, Tomasi J, Cossi M, Rega N, Millam JM, Klene M, Knox JE, Cross JB, Bakken V, Adamo C, Jaramillo J, Gomperts R, Stratmann RE, Yazyev O, Austin AJ, Cammi R, Pomelli C, Ochterski JW, Martin RL, Morokuma K, Zakrzewski VG, Voth GA, Salvador P, Dannenberg JJ, Dapprich S, Daniels AD, Farkas O, Foresman JB, Ortiz JV, Cioslowski J, Fox D. J. Gaussian 09W Revision D.01. Gaussian, Inc. Wallingford CT. 2013.

Ganesh PS, Kim SY, Kaya S, Salim R, Shimoga G, Lee SH. Quantum chemical studies and electrochemical investigations of polymerized brilliant blue-modified carbon paste electrode for in vitro sensing of pharmaceutical samples. Chemosensors. 2021a;9(6):135. https://doi.org/10.3390/chemosensors9060135.

Ganesh PS, Shimoga G, Kim SY, Lee SH, Kaya S, Salim R. Quantum chemical studies and electrochemical investigations of pyrogallol red modified carbon paste electrode fabrication for sensor application. Microchem J. 2021b;167: 106260. https://doi.org/10.1016/j.microc.2021.106260.

Ganesh PS, Shimoga G, Lee SH, Kim SY, Ebenso EE. Simultaneous electrochemical sensing of dihydroxy benzene isomers at cost-effective allura red polymeric film modified glassy carbon electrode. J Anal Sci Technol. 2021c;12:20. https://doi.org/10.1186/s40543-021-00270-w.

Garcia SM, Wong A, Khan S, Sotomayor MDPT. A simple, sensitive and efficient electrochemical platform based on carbon paste electrode modified with Fe_3O_4@MIP and graphene oxide for folic acid determination in different matrices. Talanta. 2021;229: 122258. https://doi.org/10.1016/j.talanta.2021.122258.

GaussView 6.0.16, Gaussian Inc., Wallingford CT, 2016.

Gazquez JL, Cedillo A, Vela A. Electrodonating and electroaccepting powers. J Phys Chem A. 2007;111(10):1966–70. https://doi.org/10.1021/jp065459f.

Giron AJ, Meras ID, Pena AM, Mansilla AE, Canada FC, Olivieri AC. Photoinduced fluorometric determination of folic acid and 5-methyltetrahydrofolic acid in serum using the kinetic evolution of the emission spectra accomplished with multivariate second-order calibration methods. Anal Bioanal Chem. 2008;391:827–35. https://doi.org/10.1007/s00216-008-1840-3.

Goldstein M. Enzymes controlling the biosynthesis of catecholamines. Neuroblastomas, Springer. 1966;2:66–70. https://doi.org/10.1007/978-3-642-94971-5_11.

Gomez B, Likhanova NV, Domínguez-Aguilar MA, Martínez-Palou R, Vela A, Gazquez JL. Quantum chemical study of the inhibitive properties of 2-pyridyl-azoles. J Phys Chem B. 2006;110(18):8928–34. https://doi.org/10.1021/jp057143y.

Gowda JI, Mallappa M, Nandibewoor ST. CTAB functionalized multiwalled carbon nanotube composite modifiedelectrode for the determination of 6-mercaptopurine. Sens Biosens Res. 2017;12:1–7. https://doi.org/10.1016/j.sbsr.2016.11.002.

Gowri VM, John SA. Fabrication of electrically conducting graphitic carbon nitride film on glassy carbon electrode with the aid of amine groups for the determination of an organic pollutant. J Electroanal Chem. 2020;879:114787. https://doi.org/10.1016/j.jelechem.2020.114787.

Grimme S, Ehrlich S, Goerigk L. Effect of the damping function in dispersion corrected density functional theory. J Comp Chem. 2011;32(7):1456–65. https://doi.org/10.1002/jcc.21759.

Grimme S. Semiempirical GGA-type density functional constructed with a long-range dispersion correction. J Comp Chem. 2006;27(15):1787–99. https://doi.org/10.1002/jcc.20495.

Hanabaratti RM, Tuwar SM, Nandibewoor ST, Gowda JI. Fabrication and characterization of zinc oxide nanoparticles modified glassy carbon electrode for sensitive determination of paracetamol. Chem Data Collect. 2020;30:100540. https://doi.org/10.1016/j.cdc.2020.100540.

Huang T, Chen Y, Yang B, Yang J, Wahlqvist ML, Li D. Meta-analysis of B vitamin supplementation on plasma homocysteine, cardiovascular and all-cause mortality. Clin Nutr. 2012;31(4):448–54. https://doi.org/10.1016/j.clnu.2011.01.003.

Islam N, Kaya S. Conceptual density functional theory and its application in the chemical domain. First edition. CRC Press. 2018.

Jacob JM, Kurup MRP, Nisha K, Serdaroğlu G, Kaya S. Mixed ligand copper(II) chelates derived from an O, N, S- donor tridentate thiosemicarbazone: synthesis, spectral aspects, FMO, and NBO analysis. Polyhedron. 2020;189:114736. https://doi.org/10.1016/j.poly.2020.114736.

Jiang L, Gu S, Ding Y, Ye D, Zhang Z, Zhang F. Amperometric sensor based on tricobalt tetroxide nanoparticles–graphene nanocomposite film modified glassy carbon electrode for determination of tyrosine. Colloids Surf B. 2013;107:146–51. https://doi.org/10.1016/j.colsurfb.2013.01.077.

Kingsley MP, Desai PB, Srivastava AK. Simultaneous electro-catalytic oxidative determination of ascorbic acid and folic acid using Fe_3O_4 nanoparticles modified carbon paste electrode. J Electroanal Chem. 2015;741:71–9. https://doi.org/10.1016/j.jelechem.2014.12.039.

Koopmans T. Über die Zuordnung von Wellenfunktionen und Eigenwerten zu den Einzelnen Elektronen Eines Atoms. Physica. 1934;1(1–6):104–13. https://doi.org/10.1016/S0031-8914(34)90011-2.

Krishnan R, Binkley JS, Seeger R, Pople JA, Self-consistent molecular orbital methods. 20. Basis set for correlated wave-functions. J Chem Phys. 1980;72;650–654. https://doi.org/10.1063/1.438955

Kumara M, Swamy BEK, Reddy S, Zhao W, Chetana S, Kumar VG. ZnO/functionalized MWCNT and Ag/functionalized MWCNT modified carbon paste electrodes for the determination of dopamine, paracetamol and folic acid. J Electroanal Chem. 2019;835:96–105. https://doi.org/10.1016/j.jelechem.2019.01.019.

Lee C, Yang W, Parr RG. Development of the Colle-Salvetti correlation-energy formula into a functional of the electron density. Phys Rev B. 1988;37:785–9. https://doi.org/10.1103/PhysRevB.37.785.

Lovander MD, Lyon JD, Parr DL IV, Wang J, Parke B, Leddy J. Review-electrochemical properties of 13 vitamins: a critical review and assessment. J Electrochem Soc. 2018;165(2):G18–49. https://doi.org/10.1149/2.1471714jes.

Maleh HK, Karimi F, Rezapour M, Bijad M, Farsi M, Beheshti A, Shahidi SA. Carbon paste modified electrode as powerful sensor approach determination of food contaminants, drug ingredients, and environmental pollutants: a review. Curr Anal Chem. 2019;15(4):410–22. https://doi.org/10.2174/1573411014666181026100037.

Manjunatha JG, Raril C, Hareesha N, Charithra MM, Pushpanjali PA, Tigari G, Ravishankar DK, Mallappaji SC, Gowda J. Electrochemical fabrication of poly (niacin) modified graphite paste electrode and its application for the detection of riboflavin. The Open Chemical Engineering Journal. 2020;14:90–8. https://doi.org/10.2174/1874123102014010090.

Manjunatha JG, Swamy BEK, Shreenivas MT, Mamatha GP. Selective determination of dopamine in the presence of ascorbic acid using a poly (nicotinic acid) modified carbon paste electrode. Anal Bioanal Electrochem. 2012;4(3):225–37.

Mary YS, Mary YS, Serdaroğlu G, Sarojini BK. Conformational analysis and quantum descriptors of two bifonazole derivatives of immense anti-tuber potential by using vibrational spectroscopy and molecular docking studies. Struct Chem. 2021;32:859–67. https://doi.org/10.1007/s11224-020-01678-7.

McLean AD, Chandler GS. Contracted Gaussian-basis sets for molecular calculations. 1. second row atoms, Z=11–18. J Chem Phys. 1980;72;5639–5648. https://doi.org/10.1063/1.438980

Nagaraja P, Vasantha RA, Yathirajan HS. Spectrophotometric determination of folic acid in pharmaceutical preparations by coupling reactions with iminodibenzyl or 3 aminophenol or sodium molybdate–pyrocatechol. Anal Biochem. 2002;307(2):316–21. https://doi.org/10.1016/S0003-2697(02)00038-6.

Narayana PV, Reddy TM, Gopal P, Reddy MM, Naidu GR. Electrocatalytic boost up of epinephrine and its simultaneous resolution in the presence of serotonin and folic acid at poly(serine)/multi-walled carbon nanotubes composite modified electrode: A voltammetric study. Mater Sci Eng C. 2015;56:57–65. https://doi.org/10.1016/j.msec.2015.06.011.

Nie T, Lu L, Bai L, Xu J, Zhang K, Zhang O, Wen Y, Wu L. Simultaneous determination of folic acid and uric acid under coexistence of l-ascorbic acid using a modified electrode based on poly(3,4 ethylenedioxythiophene) and functionalized single walled carbon nanotubes composite. Int J Electrochem Sci. 2013;8:7016–29.

Nunez C, Arancibia V, Trivino JJ. A new strategy for the modification of a carbon paste electrode with carrageenan hydrogel for a sensitive and selective determination of arsenic in natural waters. Talanta. 2018;187:259–64. https://doi.org/10.1016/j.talanta.2018.05.028.

Ojani R, Raoof JB, Zamani S. Electrocatalytic oxidation of folic acid on carbon paste electrode modified by nickel ions dispersed into Poly(o-anisidine) film. Electroanalysis. 2009;21(24):2634–9. https://doi.org/10.1002/elan.200904673.

Parr RG, Pearson RG. Absolute hardness: companion parameter to absolute electronegativity. J Am Chem Soc. 1983;105:7512–6. https://doi.org/10.1021/ja00364a005.

Parr RG, Szentpaly LV, Liu S. Electrophilicity index. J Am Chem Soc. 1999;121(9):1922–4. https://doi.org/10.1021/ja983494x.

Pearson RG. Absolute electronegativity and hardness correlated with molecular orbital theory. Proc Natl Acad Sci USA. 1989;83(22):8440–1. https://doi.org/10.1073/pnas.83.22.8440.

Prasad PR, Naidoo EB, Sreedhar NY. Electrochemical preparation of a novel type of C-dots/ZrO_2 nanocomposite onto glassy carbon electrode for detection of organophosphorus pesticide. Arabian J Chem. 2019;12(8):2300–9. https://doi.org/10.1016/j.arabjc.2015.02.012.

Pushpanjali PA, Manjunatha JG, Tigari G, Fattepur S. Poly(niacin) based carbon nanotube sensor for the sensitive and selective voltammetric detection of vanillin with caffeine. Anal Bioanal Electrochem. 2020;12(4):553–68.

Reed AE, Curtiss LA, Weinhold F. Intermolecular interactions from a natural bond orbital, donor-acceptor viewpoint. Chem Rev. 1988;88(6):899–926. https://doi.org/10.1021/cr00088a005.

Reed AE, Weinhold F. Natural localized molecular orbitals. J Chem Phys. 1985;83:1736–40. https://doi.org/10.1063/1.449360.

Reed AE, Weinstock RB, Weinhold F. Natural-population analysis. J Chem Phys. 1985;83:735–46. https://doi.org/10.1063/1.449486.

Selcuk O, Erkmen C, Palabiyik BB, Uslu B. Electroanalytical investigation and simultaneous determination of etodolac and thiocolchicoside at a non-modified glassy carbon electrode in anionic surfactant media. Electroanalysis. 2021;33(5):1290–8. https://doi.org/10.1002/elan.202060623.

Serdaroğlu G, Uludağ N, Ercag E, Sugumar P, Rajkumar P. Carbazole derivatives: synthesis, spectroscopic characterization, antioxidant activity, molecular docking study, and the quantum chemical calculations. J Mol Liq. 2021;330: 115651. https://doi.org/10.1016/j.molliq.2021.115651.

Serdaroğlu G. DFT and Ab initio computational study on the reactivity sites of the GABA and its agonists, Such as CACA, TACA, DABA, and Muscimol: in the gas phase and dielectric media. Int J Quantum Chem. 2011;111(14):3938–48. https://doi.org/10.1002/qua.22809.

Serdaroğlu G. Harmine derivatives: a comprehensive quantum chemical investigation of the structural, electronic (FMO, NBO, and MEP), and spectroscopic (FT-IR and UV–Vis) properties. Res Chem Intermed. 2020;46:961–82. https://doi.org/10.1007/s11164-019-04020-x.

Setoudeh N, Jahani S, Kazemipour M, Foroughi MM, Nadiki HH. Zeolitic imidazolate frameworks and cobalt-tannic acid nanocomposite modified carbon paste electrode for simultaneous determination of dopamine, uric acid, acetaminophen and tryptophan: Investigation of kinetic parameters

of surface electrode and its analytical performance. J Electroanal Chem. 2020;863: 114045. https://doi.org/10.1016/j.jelechem.2020.114045.
Sharp M, Petersson M, Edstrom K. Preliminary determinations of electron transfer kinetics involving ferrocene covalently attached to a platinum surface. J Electroanal Chem. 1979;95(1):123–30. https://doi.org/10.1016/S0022-0728(79)80227-2.
Sultan S, Shah A, Khan B, Qureshi R, Al-Mutawah JI, Shah MR, Shah AH. Simultaneous ultrasensitive detection of toxic heavy metal ions using bis(imidazo[4,5-f][1,10]phenanthroline) appended bis-triazolo Calix[4] Arene (8)/glassy carbon electrode. J Electrochem Soc. 2019;166(16):B1719–26. https://doi.org/10.1149/2.0541916jes.
Tanuja SB, Swamy BEK, Pai KV. Electrochemical determination of paracetamol in presence of folic acid at nevirapine modified carbon paste electrode: a cyclic voltammetric study. J Electroanal Chem. 2017;798:17–23. https://doi.org/10.1016/j.jelechem.2017.05.025.
Teradale AB, Lamani SD, Ganesh PS, Swamy BEK, Das SN. Niacin film coated carbon paste electrode sensor for the determination of epinephrine in presence of uric acid: a cyclic voltammetric study. Anal Chem Lett. 2017;7(6):748–64. https://doi.org/10.1080/22297928.2017.1396917.
Toriello HV. Folic acid and neural tube defects. Genet Med. 2005;7:283–4. https://doi.org/10.1097/00125817-200504000-00009.
Wang J. Analytical electrochemistry VCH publishers. New York: NY, USA; 1994.
Wei S, Zhao F, Xu Z, Zeng B. Voltammetric determination of folic acid with a multi-walled carbon nanotube-modified gold electrode. Microchim Acta. 2006;152:285–90. https://doi.org/10.1007/s00604-005-0437-1.
Ye W, Li Y, Wang J, Li B, Cui Y, Yang Y, Qian G. Electrochemical detection of trace heavy metal ions using a Ln-MOF modified glass carbon electrode. J Solid State Chem. 2020;281: 121032. https://doi.org/10.1016/j.jssc.2019.121032.
Young JE, Matyska MT, Pesek JJ. Liquid chromatography/mass spectrometry compatible approaches for the quantitation of folic acid in fortified juices and cereals using aqueous normal phase conditions. J Chromatogr A. 2011;1218(15):2121–6. https://doi.org/10.1016/j.chroma.2010.09.025.
Yuan MM, Zou J, Huang ZN, Peng DM, Yu JG. PtNPs-GNPs-MWCNTs-beta-CD nanocomposite modified glassy carbon electrode for sensitive electrochemical detection of folic acid. Anal Bioanal Chem. 2020;412(11):2551–64. https://doi.org/10.1007/s00216-020-02488-w.
Zhang D, Ouyang X, Ma W, Li L, Zhang Y. Voltammetric determination of folic acid using adsorption of methylene blue onto electrodeposited of reduced graphene oxide film modified glassy carbon electrode. Electroanalysis. 2016;28(2):312–9. https://doi.org/10.1002/elan.201500348.

Publisher's Note

Springer Nature remains neutral with regard to jurisdictional claims in published maps and institutional affiliations.

Submit your manuscript to a SpringerOpen journal and benefit from:

- ► Convenient online submission
- ► Rigorous peer review
- ► Open access: articles freely available online
- ► High visibility within the field
- ► Retaining the copyright to your article

Submit your next manuscript at ► springeropen.com